Received: 8 June 2022 | Revised: 13 September 2022 | Accepted: 16 September 2022

DOI: 10.1111/cas.15606

Cancer Science WILEY

ORIGINAL ARTICLE

Molecular subtyping of small-cell lung cancer based on mutational signatures with different genomic features and therapeutic strategies

Haiyong Wang[1] | Shuangxiu Wu[2] | Zhenzhen Li[3] | Chenyue Zhang[4] | Xiaoling Shang[5] | Chenglong Zhao[6] | Zhenxiang Li[7] | Jiamao Lin[8] | Jun Guo[1] | Zhehai Wang[1]

[1]Department of Internal Medicine-Oncology, Shandong Cancer Hospital and Institute, Shandong First Medical University and Shandong Academy of Medical Sciences, Jinan, China

[2]Division of Clinical Research, Berry Oncology Corporation, Beijing, China

[3]Division of Bioinformation, Berry Oncology Corporation, Beijing, China

[4]Department of Integrated Therapy, Fudan University Shanghai Cancer Center, Shanghai Medical College, Shanghai, China

[5]Department of Clinical Laboratory, Shandong University, Jinan, China

[6]Department of Pathology, The First Affiliated Hospital of Shandong First Medical University and Shandong Provincial Qianfoshan Hospital, Jinan, China

[7]Department of Radiation Oncology, Shandong Cancer Hospital and Institute, Shandong First Medical University and Shandong Academy of Medical Sciences, Jinan, China

[8]Department of Traditional Chinese Medicine, Shandong Cancer Hospital and Institute, Shandong First Medical University and Shandong Academy of Medical Sciences, Jinan, China

Correspondence
Zhehai Wang and Haiyong Wang, Department of Internal Medicine Oncology, Shandong Cancer Hospital and Institute, Shandong First Medical University and Shandong Academy of Medical Sciences, No. 440 Ji Yan Road, Jinan 250117, China.
Emails: badgood007@126.com (Z.W.); wanghaiyong6688@126.com (H.W.)

Funding information
Academic Promotion Program of Shandong First Medical University, Grant/Award Number: 2019RC004; Taishan Scholar Project of Shandong Province, Grant/Award Number: tsqn201812149; China Lung Cancer Immunotherapy Research Foundation

Abstract

Small-cell lung cancer (SCLC) is an exceptionally lethal malignancy characterized by extremely high alteration rates and tumor heterogeneity, which limits therapeutic options. In contrast to non-small-cell lung cancer that develops rapidly with precision oncology, SCLC still remains outside the realm of precision medicine. No recurrent and actionable mutations have been detected. Additionally, a paucity of substantive tumor specimens has made it even more difficult to classify SCLC subtypes based on genetic background. We therefore carried out whole-exome sequencing (WES) on the largest available Chinese SCLC cohort. For the first time, we partitioned SCLC patients into three clusters with different genomic alteration profiles and clinical features based on their mutational signatures. We showed that these clusters presented differences in intratumor heterogeneity and genome instability. Moreover, a wide existence of mutually exclusive gene alterations, typically within similar biological functions, was

Abbreviations: AI, allelic imbalance; BER, base excision repair; CNV, copy number variation; CPF, cleavage and polyadenylation factor; DDR, DNA damage repair; FA, Fanconi anemia; FDR, false discovery rate; FFPE, formalin-fixed and paraffin-embedded; FGA, fractions of genome altered; GISTIC, Genome Identification of Significant Targets in Cancer; HLA, human leukocyte antigen; HPD, hyperprogressive disease; HRR, homologous recombination repair; ICI, immune checkpoint inhibitor; indel, insertion and deletion; ITH, intratumor heterogeneity; LOH, loss of heterozygosity; MAD, median absolute deviation; MATH, mutant allele tumor heterogeneity; MMR, mismatch repair; NSCLC, non-small-cell lung cancer; OS, overall survival; PD-L1, programmed cell death-ligand 1; SCH, Shandong Cancer Hospital and Institute; SCLC, small-cell lung cancer; SNV, single nucleotide variation; TGF-β, transforming growth factor-β; TIL, tumor-infiltrating lymphocyte; TMB, tumor mutation burden; TNB, tumor neoantigen burden; VAF, variant allele frequency; WBC, white blood cell; WES, whole-exome sequencing; WGD, whole genome doubling; WGS, whole-genome sequencing.

detected and suggested a high SCLC intertumoral heterogeneity. Particularly, Cluster 1 presented the greatest potential to benefit from immunotherapy, and Cluster 3 constituted recalcitrant SCLC, warranting biomarker-directed drug development and targeted therapies in clinical trials. Our study would provide an in-depth insight into the genome characteristics of the Chinese SCLC cohort, defining distinct molecular subtypes as well as subtype-specific therapies and biomarkers. We propose tailoring differentiated therapies for distinct molecular subgroups, centering on a personalized precision chemotherapy strategy combined with immunization or targeted therapy for patients with SCLC.

KEYWORDS
small-cell lung cancer, somatic mutational signature, subtype classification, therapeutic strategy, whole-exome sequencing

1 | INTRODUCTION

Small-cell lung cancer accounts for approximately 15% of lung cancer. Due to its elusive nature, minimal improvements have been made in SCLC treatments in recent years, rendering it a recalcitrant disease.[1] Recently, immunotherapy has brought hope to SCLC patients.[2] However, prolongations in progression-free survival and OS for SCLC patients are limited and modest, with a vast majority of patients experiencing drug resistance and disease recurrence.[3,4] Non-small-cell lung cancer has entered a precision therapy era under the guidance of driving genes and achieved great success, whereas SCLC is still in the traditional unselective treatment era. In addition, SCLC is rarely treated by surgery and few specimens are available for genomic characterization. Therefore, a deeper understanding of SCLC genetic properties is required to guide new treatment strategies.

Recently, some progress has been made in the exploration of SCLC patients' treatments. It has been proposed that SCLC can be classified into four major subtypes: SCLC-A, SCLC-N, SCLC-P, and SCLC-Y, distinguished by *ASCL1*, *NeuroD1*, *POU2F3*, and *YAP1* transcriptional regulators, respectively.[5] Further studies have updated an inflamed SCLC subtype, SCLC-I, which is not defined by *YAP1* expression.[6] It is worth noting that, traditionally, SCLC subgroups were believed to not be distinguished by genetic characteristics. Theoretically, SCLC genomic hallmarks, biallelic loss of *RB1* and *TP53*, are so prevalent that they cannot be used to define subclasses.[7] Additionally, there is not a large number of sample sequencing data available, so it is even more difficult to classify SCLC subtypes based on genetic landscape. However, a comprehensive analysis of SCLC's genetic characteristics is crucial for the discovery of driving genes and new subtype definitions, which will directly guide individualized treatments. Moreover, previous studies involving the *MYC* and *NOTCH* families reported the feasibility and importance of gene-driven individualized therapy for SCLC.[8,9] Therefore, the description of SCLC molecular subtypes based on genomic characteristics is required.

In our current study, we proposed three SCLC molecular classifications based on mutational signatures by WES among a Chinese cohort. Data from 178 SCLC patients were collected from SCH, the largest genome-sequencing study on Chinese SCLC to date. We analyzed the differences between the three molecular classifications in SNV, CNV, genomic instability, and immunity, and proposed an individualized treatment strategy. Our study provide an in-depth insight into the genome characteristics of the Chinese SCLC cohort, defining distinct molecular subtypes as well as subtype-specific therapies and biomarkers. It also represents an important step forward to tailor optimal and personalized treatments for SCLC patients.

2 | MATERIALS AND METHODS

2.1 | Sample collection, processing, and genomic DNA extraction

We recruited histologically confirmed SCLC patients from SCH. All diagnoses were independently confirmed by two experienced pathologists. In addition to blood samples (2 ml), tumor tissue samples were obtained by biopsies. A strict quality inspection was undertaken to remove contaminated and insufficient DNA samples. Finally, 178 patients were enrolled. The OS was defined as the interval between diagnosis and death/the last observation point. For surviving patients, data were censored at the last follow-up (26 November 2020). Clinicopathologic data were retrieved. This study was approved by the Ethics Committee of the SCH. All patients included in this study provided written informed consent.

Biopsied tumor tissues were fixed with formalin, then embedded in paraffin. Corresponding blood samples were set as controls. Genomic DNA was extracted from each FFPE sample using the GeneRead DNA FFPE Kit (Qiagen) and from the blood sample using the DNA Blood Midi/Mini kit (Qiagen).

2.2 | DNA library construction and WES, data processing, and alignment

The detailed procedures are provided in Appendix S1.

2.3 | Public data of Caucasian SCLC patients

The WES mutation files of 45 Caucasian SCLC patients were retrieved from George et al[8] data that used a Caucasian SCLC cohort for somatic mutational signature and alteration frequency analyses. The Caucasian ancestry of these patients was confirmed according to their clinical information.

2.4 | Mutational signature analysis

Somatic mutational signatures were de novo analyzed from the clean WES data by the "Somatic Signatures" R package (version 2.20.0),[10] according to a non-negative matrix factorization. Four highly confident mutational signatures were derived in the SCH cohort. They were then compared with the consensus signatures in the COSMIC dataset (https://cancer.sanger.ac.uk/cosmic/), based on the Cosine similarity analysis to nominate each derived signature with the highest COSMIC dataset similarity (i.e. SBS4 [S4], SBS2 [S2], SBS6 [S6] and SBS5 [S5]) for the SCH cohort.

To further determine mutational signatures' distribution and frequencies of each patient, deconstructSigs (version 1.9.0) was used as previously described.[11] Patients harboring S2, S4, S5, and S6 mutations, as well as S2, S4, S5, and S6 weights in clonal and subclonal mutations, were compared using the Wilcoxon rank-sum test between two clusters and Kruskal–Wallis test among the three clusters. Correlations between signatures and categorical clinical feature variables were undertaken as described in Appendix S1.

2.5 | Mutational signature clustering for SCLC subgroup classification

Mutational signatures of each patient were considered to determine SCLC subgroups in the SCH cohort, based on the four mutational signatures' weights in each patient using "Ward. D2's method" R package based on maximum distance.[12]

2.6 | Somatic mutation variants detection and driver gene prediction

Somatic SNVs were identified from clean sequencing data by MuTect[13] and somatic small indels were detected by GATK Somatic Indel Detector. The ANNOVAR software was used for variants annotation based on multiple databases as previously described.[14] After annotation, the retained nonsynonymous SNVs were screened from disease databases for further analysis with VAF (cut-off ≥3%) or VAF for cancer hotspots (cut-off ≥1%). Tumor mutation burden was calculated with the total numbers of nonsynonymous SNVs and indel variants per megabase of coding regions. Dominant tumor neoantigens were predicted using OptiType to infer the individual HLA type.[15] Tumor neoantigen burden was calculated with the total numbers of neoantigens per megabase of coding regions. Significant driver genes were identified by combining MutsigCV and dNdScv, as previously described,[16,17] with an FDR cut-off <5%.

2.7 | Copy number variation identification

Copy number variations, for all patients on the SCH cohort, were first identified using the GISTIC 2.0 algorithm.[18] At the chromosomal arm-level, significant amplifications or deletions were screened with FDR (cut-off <10%) for further analyses. At a focal CNV level, significant amplification was screened with FDR (cut-off <5%) and G-score (cut-off >0.3). Significant deletion was screened with FDR (cut-off <5%) and G-score (cut-off <−0.2) for further analyses.

Focal CNV-related gene analysis was undertaken for each patient based on paired tumor–normal WES data using GATK. Then focal CNV-related genes were filtered according to the COSMIC cancer gene census database (https://cancer.sanger.ac.uk/cosmic/) to obtain a cancer-related focal CNV gene list.

2.8 | Pathway and functional enrichment analysis

Somatic mutation and focal CNV-related genes that enriched biological functions and involved pathways were analyzed using the online tool metascape (https://metascape.org/gp/index.html#/main/step1), based on the Gene Ontology (GO) and Kyoto Encyclopedia of Genes and Genomes (KEGG) databases (https://www.kegg.jp/kegg/kegg1.html).

Somatic mutations and focal CNV-related genes were evaluated by canonical oncogenic signaling and DDR pathways mapping, according to the templates from The Cancer Genome Atlas Pan-Cancer Atlas project.[19,20] A pathway was considered "altered" when it contained equal to or more than 1 gene altered in a specimen. The number of oncogenic signaling or DDR pathway alterations of each specimen was also calculated.

2.9 | Tumor heterogeneity and genome instability analysis

To investigate ITH, MATH values for each tumor sample were calculated from the MAD and the median of its mutant-allele fractions at tumor-specific mutated loci: MATH = 100×MAD/median. Detailed information can be found in Appendix S1.

2.10 | Immunohistochemical staining, PD-L1 expression, and $CD8^+$ T cell infiltration

The detailed procedures are reported in Appendix S1.

2.11 | Statistical analyses

The R Foundation for Statistics Computing Package (R package, version 3.3.3) was used. Fisher's exact test (for somatic mutation genes, CNV-related genes, and pathway alterations) and the Wilcoxon rank–sum test were used to analyze the relationships between clusters. The Kruskal–Wallis test was used to examine trends among the three clusters. The Kaplan–Meier test was used to estimate effects on OS based on log–rank tests. A p value less than 0.05 was considered statistically significant. Hazard ratios of multiple factors on OS were obtained from the Cox proportional hazards model.

3 | RESULTS

3.1 | Research design

As illustrated in Figure S1, WES was carried out on FFPE specimens of primary lung tumor (n = 145), lymph node (n = 30), and other (n = 3) biopsies and matched WBC (n = 178). Whole exome sequencing had an average sequencing depth of 362× (range, 216–570) for tumor tissues and 182× (range, 116–274) for WBCs. The mean genomic coverage of ≥20 reads was 97.7% (Table S1).

3.2 | Small-cell lung cancer subtype molecular classification based on somatic mutational signatures and their distinct prognostic and clinical features

Mutational signatures were de novo calculated and characterized from 178 specimens based on the 96 possible mutation types (Figure S2A), according to a previously published method.[10,11,21] Four highly-confident signatures were derived and compared to the COSMIC mutational signature database: smoking-related S4 (97.2% of similarity), AID/APOBEC family-related S2 (72.5%), MMR-related S6 (75.5%), and unknown S5 (84.3%) (Figure S2B). Based on four mutational signature proportions in each sample and using unsupervised clustering, patients were divided into three clusters: cluster 1 (n = 47; 26.4%); cluster 2 (n = 50; 28.1%); and cluster 3 (n = 81; 45.5%) (Figure 1A and Table S2A). Each somatic mutation signature weight was significantly different between clusters. Cluster 1 mostly presented S4 mutations (median = 0.70 [range, 0.56–0.93]) and had the lowest proportion of S2 mutations (median = 0 [0.0–0.1]). Cluster 3 mostly harbored S5 mutations (median = 0.48 [range, 0.0–0.76]), followed by similar proportions of S6 (median = 0.24 [range, 0.0–0.79]) and S4 (median = 0.2 [range, 0.0–0.42]), and lower S2 (median = 0.07 [range, 0.0–0.31]}. Cluster 2 presented an intermediary profile between clusters 1 and 3 (Figure 1B). Consistent results were observed on the clonal and subclonal somatic mutations analysis between the three clusters, except for the S6 weight, that increased in all subclonal mutations (Figure S2C). This indicated a possible molecular change of the evolution trajectory during SCLC tumor development, and implied the presence of therapeutic vulnerabilities for different SCLC subtypes and stages. Additionally, the three clusters had distinct prognostic and clinical features. Cluster 1 had a significantly longer OS (p = 0.007 vs. cluster 2 and p = 0.0003 vs. cluster 3), while the OS of clusters 2 and 3 did not differ (p = 0.25) (Figure 1C). Cluster 1 predominantly consisted of women ($p = 7.25\times10^{-12}$), and fewer smokers ($p = 3.78\times10^{-10}$) and drinkers (p = 0.003) (Figure 1D, Table S3). Cluster 3 were predominantly male, smokers, drinkers, older (>60 years, p = 0.036), and extensive-stage patients (p = 0.008) (Figure 1D, Table S3). Specimen type and family history of cancer did not significantly differ among the three clusters (Figure S2D,F). Cox regressive analysis confirmed that cluster 1 (C1) and limited-stage were independent influence factors for longer OS times (p = 0.046 and 0.002, respectively) (Figure S2E).

Additionally, we further validated the de novo signature classification in a Caucasian SCLC cohort dataset[8] and obtained three clusters of patients. Clusters 1 and 2 presented higher proportions of S4 mutations, whereas cluster 3 harbored elevated S2 mutations and significantly less S4 mutations (Figure 1E, Table S2B). S6 mutations were not identified in the Western SCLC cohort. The OS did not significantly differ among the three clusters of Caucasian SCLC (p = 0.65) (Figure 1F). These classification differences might be derived from the small patient population in the Caucasian cohort, or different SCLC genetic alteration features between Chinese and Caucasian cohorts, which requires future studies.

3.3 | Higher TMB and lower intratumor heterogeneity in cluster 1 patients

The WES revealed 53,933 somatic nonsynonymous (nonsilent) SNVs/indels in the Chinese SCLC cohort. Cluster 1 had a median of 461 (range, 195–884), cluster 2 of 253 (range, 126–772), and cluster 3 of 187 (range, 64–726) mutations (Table S4A), suggesting the high-load somatic mutation of SCLC.[9] Except for *TMEM132D* (20.2%), a neural cell transmembrane gene that significantly recurred in cluster 2, 35 mutations recurred more frequently (≥15%) in cluster 1 compared to other clusters (Figure S3A). Furthermore, cluster 1 presented significantly higher TMB (median 11.2; range, 4.7–21.5),

FIGURE 1 Molecular classification of patients with small-cell lung cancer (SCLC) and their mutational signature and clinical features. (A,E) Classification of 178 Chinese and 45 Caucasian SCLC patients into three clusters (C1–C3), based on somatic mutational signatures. Relatively clinical features of each patient are indicated at the bottom of the graph. (B) Weights of different somatic mutational signatures in each cluster. (C,F) Survival analysis of patients in each cluster and overall survival based on log–rank test for the (C) Chinese and (F) Caucasian cohorts. (D) Comparisons of clinical features among SCLC patients among the three clusters based on the Kruskal-Wallis test. p-values <0.05 or <0.01 denote a significant or an extremely different level, respectively.

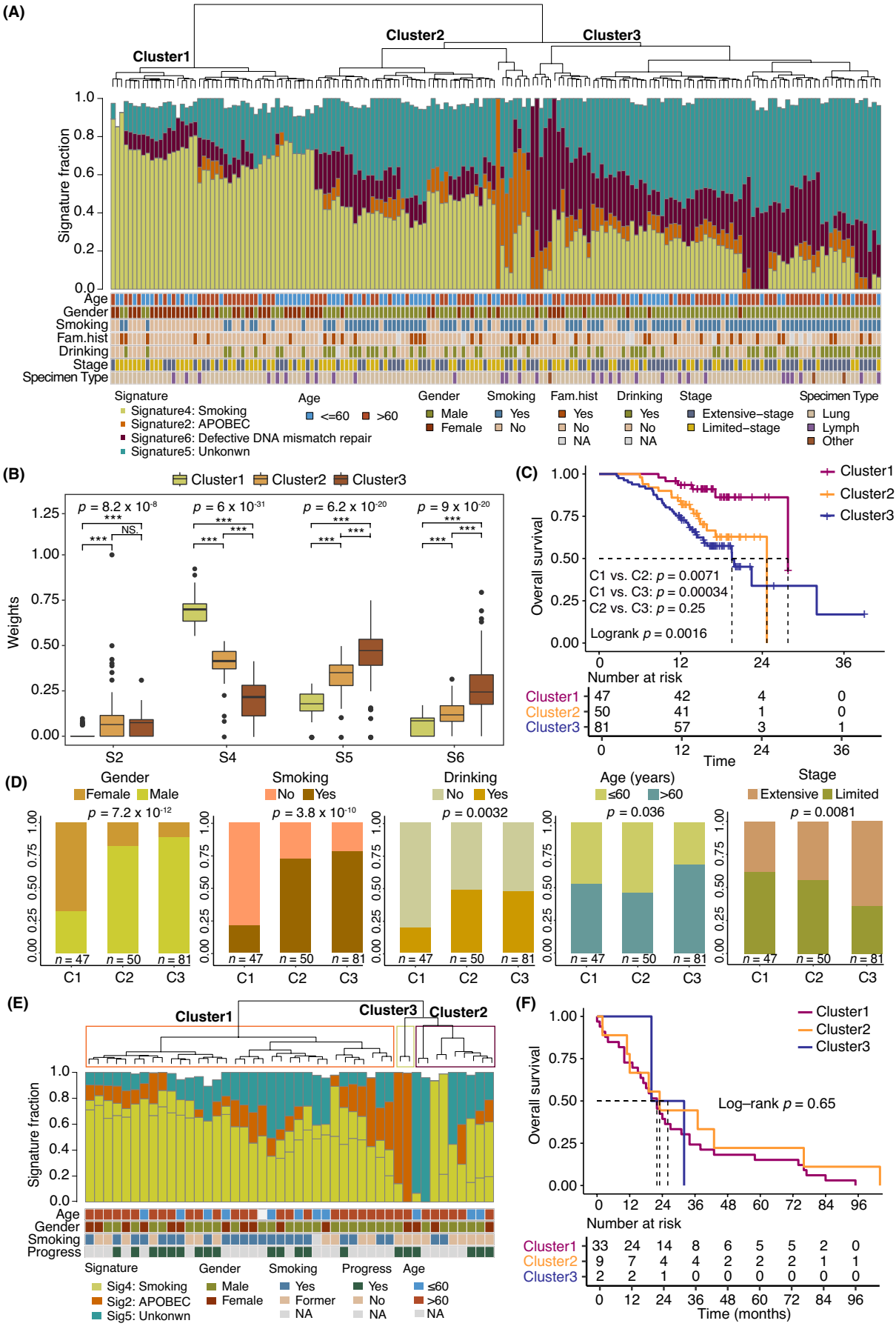
(A)
Cluster1
Cluster2
Cluster3
Signature fraction
Age
Gender
Smoking
Fam.hist
Drinking
Stage
Specimen Type
Signature
Signature4: Smoking
Signature2: APOBEC
Signature6: Defective DNA mismatch repair
Signature5: Unkonwn
Age
<=60
>60
Gender
Male
Female
Smoking
Yes
No
Fam.hist
Yes
No
NA
Drinking
Yes
No
NA
Stage
Extensive−stage
Limited−stage
Specimen Type
Lung
Lymph
Other
(B)
Cluster1 Cluster2 Cluster3
p = 8.2 x 10-8
p = 6 x 10-31
p = 6.2 x 10-20
p = 9 x 10-20
NS.
Weights
S2
S4
S5
S6
(C)
Cluster1
Cluster2
Cluster3
Overall survival
C1 vs. C2: p = 0.0071
C1 vs. C3: p = 0.00034
C2 vs. C3: p = 0.25
Logrank p = 0.0016
Number at risk
Cluster1 47 42 4 0
Cluster2 50 41 1 0
Cluster3 81 57 3 1
Time
(D)
Gender
Female Male
p = 7.2 x 10-12
Smoking
No Yes
p = 3.8 x 10-10
Drinking
No Yes
p = 0.0032
Age (years)
≤60 >60
p = 0.036
Stage
Extensive Limited
p = 0.0081
n = 47
n = 50
n = 81
C1
C2
C3
(E)
Cluster1
Cluster3
Cluster2
Signature fraction
Age
Gender
Smoking
Progress
Signature
Sig4: Smoking
Sig2: APOBEC
Sig5: Unkonwn
Gender
Male
Female
Smoking
Yes
Former
NA
Progress
Yes
No
NA
Age
≤60
>60
NA
(F)
Cluster1
Cluster2
Cluster3
Overall survival
Log−rank p = 0.65
Number at risk
Cluster1 33 24 14 8 6 5 5 2 0
Cluster2 9 7 4 4 2 2 2 1 1
Cluster3 2 2 1 0 0 0 0 0 0
Time (months)

clonal SNV/indel fraction (median 0.82; range, 0.62–0.96), and VAF (median 0.39; range, 0.03–1.0), and the lowest fraction of LOH gene regions ($p < 0.01$) (Figure 2A). This indicated that, although patients in cluster 1 had significantly higher TMB, they also had lower intratumor heterogeneity compared to other clusters, especially cluster 3.

3.4 | Driver and recurrent somatic mutation genes among the three clusters

Due to the extremely high mutation rates in SCLC genomes,[8] the abundance and heterogeneity of different unknown-significant somatic mutations hamper the definition of pathophysiological functions of those mutations in SCLC. Therefore, we used MutSigCV and dNdScv (FDR $q < 0.1$) to identify somatic mutation driver genes (Figure 2B, Table S4B). Beyond *TP53* (93.3%), *RB1* (44.4%), *KMT2D* (24.7%), *NOTCH1* (20.2%), *CREBBP* (17.9%), *TP73* (10.1%), *ARID1A* (9.6%), and *PTEN* (6.2%), previously reported as recurrent in SCLC,[8,22–25] other driver genes were predicted, and most of them recurred evenly among the three clusters in the Chinese SCH cohort. Noteworthy, as high as 54.6% inactivation mutations were observed among the predicted driver genes (Figure 2B). Approximately 81% of *TP53*, 84% of *RB1*, and 82% of *PTEN* mutations were LOH ones (Figure S3B), Table S4C), confirming a high level of biallelic inactivation in essential genes in SCLC.

These driver genes were most significantly enriched in transcription coactivator activity, transcription initiation from RNA polymerase II promoter, and protein phosphatase binding involved in functions such as regulation of cell cycle process, response to biotic stimulus, T cell proliferation, chromosome segregation regulation, and ECM structural constituents, and many fundamental cellular catabolic processes (Figure 2C). The mutations significantly impacting OS were enriched in different functions (Figure 2D, Table S4D), indicating their different crucial roles in SCLC initiation and development.

3.5 | Increased copy number variations and chromosomal instability in SCLC patients from clusters 1 to 3

Regarding chromosome level somatic CNVs, we observed significantly recurrent deletions in 3p (*ROBO1/ROBO2* at 3p12.3), 4p (*FGFR3*, 4p16.3), 5q (*FLT4*, 5q35.3), 10q (*PTEN*, 10q23.31), 13q (*RB1* and *CYSLTR2*, 13q14.2), 17p (*TP53*, 17p13.1), and 22q (*RAC2*, 22q13.1) regions, as well as amplification in 1p (Table S5). These CNVs were previously reported in Western cohorts.[5,8] Also, we used the GISTIC method and cancer-related genes in the COSMIC database and identified deletions in the 2p/q, 4q, 5p, 10p, 15q, and 16q regions with recurrent *CTNNA2*, *RGPD3*, *ZNF479*, and *LRIG3* oncogenes among the three clusters; as well as amplifications in the 1q, 3q, 12q, 17q/p, 18q/p, 19q/p, 20q/p, and 22q regions with recurrent *TERT* and *PTPN6* among the three clusters (Figure 3A and Figure S4A, Table S5A–C). Less shared CNV-amplification genes were identified in clusters 2 and 3 compared to cluster 1, indicating their higher intertumoral heterogeneity on the CNV level. More amplification of MYC family genes was identified in cluster 3, including 3.9% *MYC*, 7.9% *MYCL*, and 1.1% *MYCN*. These amplifications were lower than those reported in the Western cohort (approximately 6%–25%, 7.8%–12%, and 2%, respectively),[5,7,26] suggesting different SCLC chromosomal alteration contexts between Chinese and Western cohorts. Other MYC pathway genes, including *MNT* (6.2%), *MXD4* (6.7%), *MXD3* (2.3%), *MLX* (2.8%), *MLXIP* and *MLXIPL* (0.6%), and *MAX* (1.1%), but not *MGA* or *BRG1*, were exclusively amplified or mutated with MYC family genes (Figure S4B-4C). This demonstrated the oncogenic importance of the MYC family and pathway in SCLC tumorigenesis and development. *MAZ* amplification has been observed among the178 SCLC patients (Figure S4C).

Increasing focal CNV numbers in clusters 1–3 were observed (Figure 3B). Among all 278 significantly differential focal CNV genes (239 amplified and 39 deleted), 83.1% focal CNV genes (209 amplified and 22 deleted) predominated in cluster 3, followed by cluster 2 ($p < 0.05$; Fisher's exact test). This illustrated the higher chromosomal instability in cluster 3. The most recurrent CNV-deletion and CNV-amplification focal genes were *TBC1D3* (41%, 17q12), a tumor suppressor gene involved in calmodulin interaction and transmembrane trafficking,[27] and *MAZ* (41%, 16p11.2), a MYC-associated zinc finger protein gene (Figure S4D, Table S5A–C).[28] Particularly, the *MAZ* amplification had a significant impact on OS ($p = 0.038$, Figure 3C). However, *MAZ* and *TBC1D3* expressions and roles in SCLC have not been explored.

The amplified CNVs were enriched in nerve cellular metabolic processes and oncogenic signaling pathways. Copy number variation deletions were significantly mapped in cell adhesion molecular binding, histone modification, and structural molecular activity (Figure 3D, Table S5D). This suggested a clear difference in molecular functions and processes between CNV amplifications and deletions, which might play essential roles in SCLC development and chemotherapy resistance.

3.6 | Mutually exclusive somatic mutations and CNVs enriched in essential pathways reflected SCLC's high intertumoral heterogeneity

Based on somatic mutations and CNVs, we found a wide presence of mutually exclusive gene alterations in SCLC, not only within the same pathways but also between different ones, including 10 certain oncogenic signaling pathways[19] and eight DDR pathways[20,29] (Figure 4A and Figure S5A, S5B). It suggests that high SCLC intertumoral heterogeneity greatly hinders targeted therapy efficiency and treatment among SCLC patients. Therefore, individually functional biomarker-directed drug development and therapy strategies deserve attention.

To explore the mutational status and therapeutic potentials of essential genes in SCLC, we calculated gene alteration frequencies of 10 oncogenic signaling pathways[19] and eight DDR pathways[20,29] in our cohort (Figure 4A) and compared them among the three clusters (Figure 4B). Pathway-related SNVs/indels were mainly

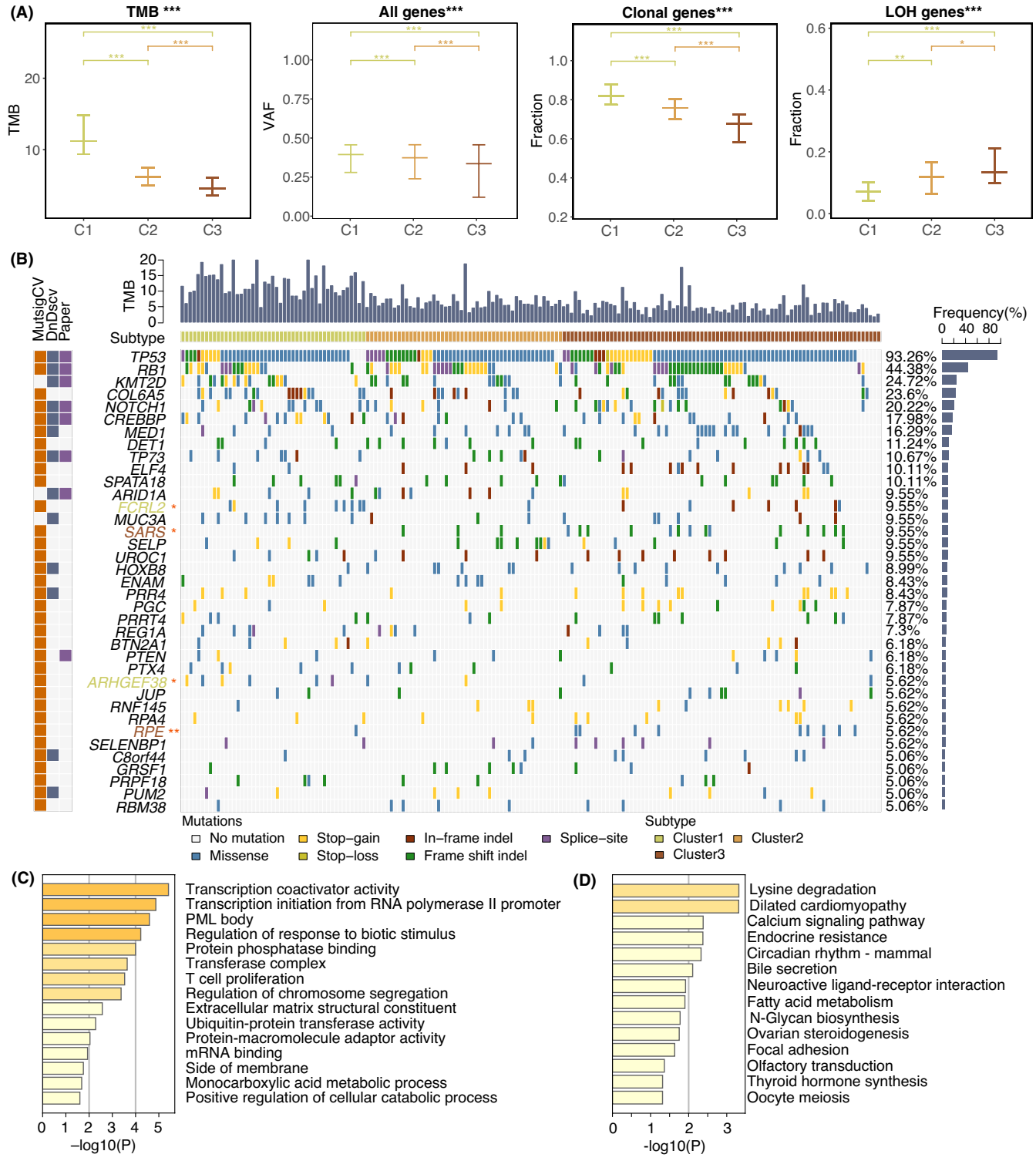

FIGURE 2 Somatic mutational features and driver genes among three clusters of Chinese patients with small-cell lung cancer (SCLC). (A) Comparison of somatic mutational features, including tumor mutation burden (TMB), proportions of clonal, all gene, and loss of heterozygosity (LOH) somatic mutation genes among the three clusters (C1–C3). (B) Driver genes predicted using MutSigCV and dNdScv (false discovery rate $q < 0.1$). Driver genes reported in previous SCLC articles are indicated as "Paper" on the left column of the graph. Differentially recurrent mutation genes among the three clusters are indicated by asterisks. Yellow, orange, and brown indicate the predominately recurrent genes in clusters 1, 2, and 3, respectively. The mutation frequency of each gene is on the right pattern and the TMB values are at the top of the graph. (C) Gene Ontology functions enriched by all the driver genes predicted in this study. (D) Kyoto Encyclopedia of Genes and Genomes pathways enriched by the somatic mutation genes that significantly affected overall survival in this study.

enriched in cluster 1 and focal CNVs were mainly enriched in cluster 3 (Figure 4A). The SNVs/indels on Notch (97.9% of cluster 1) and Wnt (76.6%) of the oncogenic signaling pathways, and FA (53.2%) and BER (53.2%) of the DDR pathways were predominant in cluster 1 ($p < 0.05$, Figure 4B). Focal CNVs of Notch (74.1% of cluster 3), Wnt (43.2%), RTK/RAS (49.4%), and Hippo (24.7%) of the oncogenic signaling pathways, and FA (43.2%), BER (42.0%), and HRR (38.3%) of the DDR pathways were significantly enriched in cluster 3, and PI3K (42.0%) was enriched in cluster 2 ($p < 0.05$; Figure 4B, Table S6). Thus, alterations of Notch (91.6% of all patients), Wnt (71.9%), FA (57.9%), HRR (52.3%), and BER (49.4%) pathways were predominant in SCLC and might be important for SCLC tumorigenesis. MYC (36.0% of all patients) and MMR (51.6%) pathway alterations might contribute to SCLC development on extended stages.

We noted that SCLC patients harboring PI3K and TGF-β pathway SNVs had longer OS (Figure 4C), indicating potential benefit from current chemotherapies. However, patients harboring NRF2 pathway SNVs, and PI3K and CPF pathway CNVs did not benefit from chemotherapies. Except for these four pathways, no relationship with OS was detected for other pathway alterations. This might be due to high intertumoral heterogeneity among SCLC patients and no suitable targeted drugs have been used. Therefore, alternative therapy regimens should be explored for SCLC patients harboring mutually exclusive genetic alterations.

3.7 | Different genome instability and epigenomic features across the three SCLC subtypes

We estimated the FGA, AI, MATH, LOH regions, ploidy, and WGD in each patient to indicate the SCLC genome instability status and compared them among the three clusters. Results showed that these parameters were at the lowest levels in cluster 1 compared to other clusters, and particularly lower compared to cluster 3 ($p < 0.05$) (Figure 5A). This was consistent with the SNV ITH analysis results (Figure 2A), which showed that the SCLC genome was relatively stable in cluster 1 patients.

Furthermore, we investigated SNV and CNV alterations related to genome organization. Top recurrent genes included somatic mutations of epigenetic regulators of the KMT2 (*KMT2D* (24.7%), *KMT2C* (11.2%), *KMT2B* (6.2%)), KMT5/6 (*KMT5B*, 10.1%), KDM (*KDM3A/B* (5.1%), *KDM4C* (5.1%), *KDM6A* (4.5%), *KDM5D* deletion (9.6%)), HAT (*CREBBP* (18.0%), *EP400* (7.9%), *EP300* (7.3%)) families, and *PRMT1* amplification (10.1%) (Table S7). These recurrent multiple epigenetic modifications on histone marks in the enhancers/promoters globally repress, or favor, transcript activation of numerous downstream oncogenes, tumor suppressor genes, and cell–cell/cell-matrix adhesion genes. Moreover, loss-of-function mutations of these genes within a family were mutually exclusive[8,9] and also observed in almost 54.5% ($n = 97/178$) of SCLC patients in our current study (Figure 5B and Figure S6A, S6B). The mutation frequencies of most of these genes did not significantly differ between the three clusters (Table S7), indicating their equivalent contributions to SCLC tumorigenesis and development. Therefore, it is important to identify the upstream factors that control these epigenetic regulation genes and downstream target genes, which can be potential therapeutic targets. For instance, the NOTCH family might be an upstream regulator for *CREBBP/EP300* in SCLC.[30]

3.8 | Immunotherapy features across the three SCLC subtypes

Immune checkpoint inhibitors have become important treatment options for SCLC. Expression of PD-L1, $CD8^+$ TILs, TMB, and TNB expressions are commonly used as predictive markers of ICI.[31,32] Besides TMB (Figure 2A) and TNB (Figure 6A), higher PD-L1 expressions were mostly present in cluster 1 ($p < 0.05$ compared to clusters 2 and 3) (Figure 6B,C). $CD8^+$ TILs are higher in cluster 1 compared to other clusters (Figure 6D). Human leukocyte antigen, a new ICI prediction biomarker, has been reported at a high heterozygosity level (HLA-I loci) on patients with improved OS after ICI, compared to HLA loci homozygosity.[33] Human leukocyte antigen heterozygosity in cluster 3 patients was significantly lower ($p < 0.05$; Figure 6E), indicating that cluster 1 patients might benefit from immunotherapy.

Some specific gene mutations have been reported to affect ICI's efficiency.[34] We identified that *FANCA*, an immunotherapy-positive gene, had a higher mutation frequency in cluster 1 ($p < 0.05$; Figure 6F). However, an immunotherapy-negative gene, *CTNNB1*, and an HPD gene, *DNMT3A*, were also identified in cluster 1 ($p < 0.05$, especially compared with cluster 3; Figure 6G,H). Therefore, it is necessary to identify whether the immunotherapy-negative and HPD gene mutations are present in SCLC patients treated with ICIs.

3.9 | Therapeutic vulnerability/strategies across the three SCLC clusters

Alteration frequencies of highly recurrent genes and significant differentially recurring genes among the three clusters, and their corresponding pathways, are indicated in Figure 7. Detailed information on therapeutic vulnerabilities targeting associated pathways are presented in Appendix S1.

FIGURE 3 Comparison of copy number variations among the three clusters of Chinese patients with small-cell lung cancer (SCLC) and their enriched biological functions. (A) Venn diagrams showing different amplification (Amp) and deletion (Del) focal copy number variation (CNV) genes among the three clusters (C1–C3) predicted by the Genome Identification of Significant Targets in Cancer method (false discovery rate $q < 0.1$). (B) Increasing focal gene numbers in SCLC patients from clusters 1 to 3. (C) Survival analysis for SCLC patients harboring *MAZ* gene amplification and overall survival (OS), compared with patients with WT. Log–rank test. MT, mutant. (D) Kyoto Encyclopedia of Genes and Genomes (KEGG) pathways and Gene Ontology (GO) functions enriched by focal CNV genes that significantly affected OS.

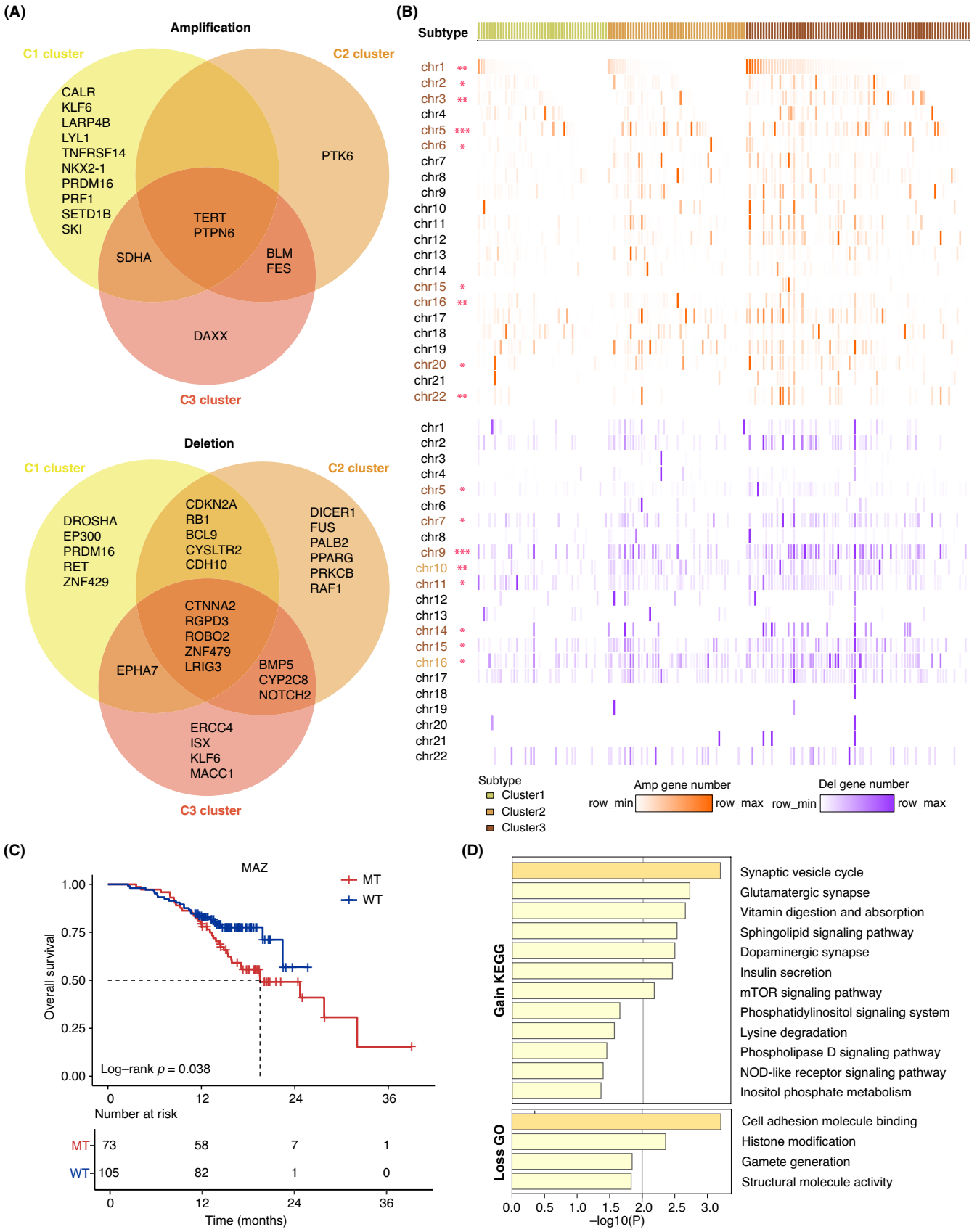
(A)
Amplification
C1 cluster
C2 cluster
C3 cluster
CALR
KLF6
LARP4B
LYL1
TNFRSF14
NKX2-1
PRDM16
PRF1
SETD1B
SKI
PTK6
TERT
PTPN6
SDHA
BLM
FES
DAXX
Deletion
C1 cluster
C2 cluster
C3 cluster
DROSHA
EP300
PRDM16
RET
ZNF429
CDKN2A
RB1
BCL9
CYSLTR2
CDH10
DICER1
FUS
PALB2
PPARG
PRKCB
RAF1
CTNNA2
RGPD3
ROBO2
ZNF479
LRIG3
EPHA7
BMP5
CYP2C8
NOTCH2
ERCC4
ISX
KLF6
MACC1
(B)
Subtype
chr1 **
chr2 *
chr3 **
chr4
chr5 ***
chr6 *
chr7
chr8
chr9
chr10
chr11
chr12
chr13
chr14
chr15 *
chr16 **
chr17
chr18
chr19
chr20 *
chr21
chr22 **
chr1
chr2
chr3
chr4
chr5 *
chr6
chr7 *
chr8
chr9 ***
chr10 **
chr11 *
chr12
chr13
chr14 *
chr15 *
chr16 *
chr17
chr18
chr19
chr20
chr21
chr22
Subtype
Cluster1
Cluster2
Cluster3
Amp gene number
row_min
row_max
Del gene number
row_min
row_max
(C)
MAZ
MT
WT
Overall survival
1.00
0.75
0.50
0.25
0.00
Log–rank p = 0.038
0
12
24
36
Number at risk
MT 73 58 7 1
WT 105 82 1 0
Time (months)
(D)
Gain KEGG
Synaptic vesicle cycle
Glutamatergic synapse
Vitamin digestion and absorption
Sphingolipid signaling pathway
Dopaminergic synapse
Insulin secretion
mTOR signaling pathway
Phosphatidylinositol signaling system
Lysine degradation
Phospholipase D signaling pathway
NOD-like receptor signaling pathway
Inositol phosphate metabolism
Loss GO
Cell adhesion molecule binding
Histone modification
Gamete generation
Structural molecule activity
0.0
0.5
1.0
1.5
2.0
2.5
3.0
–log10(P)

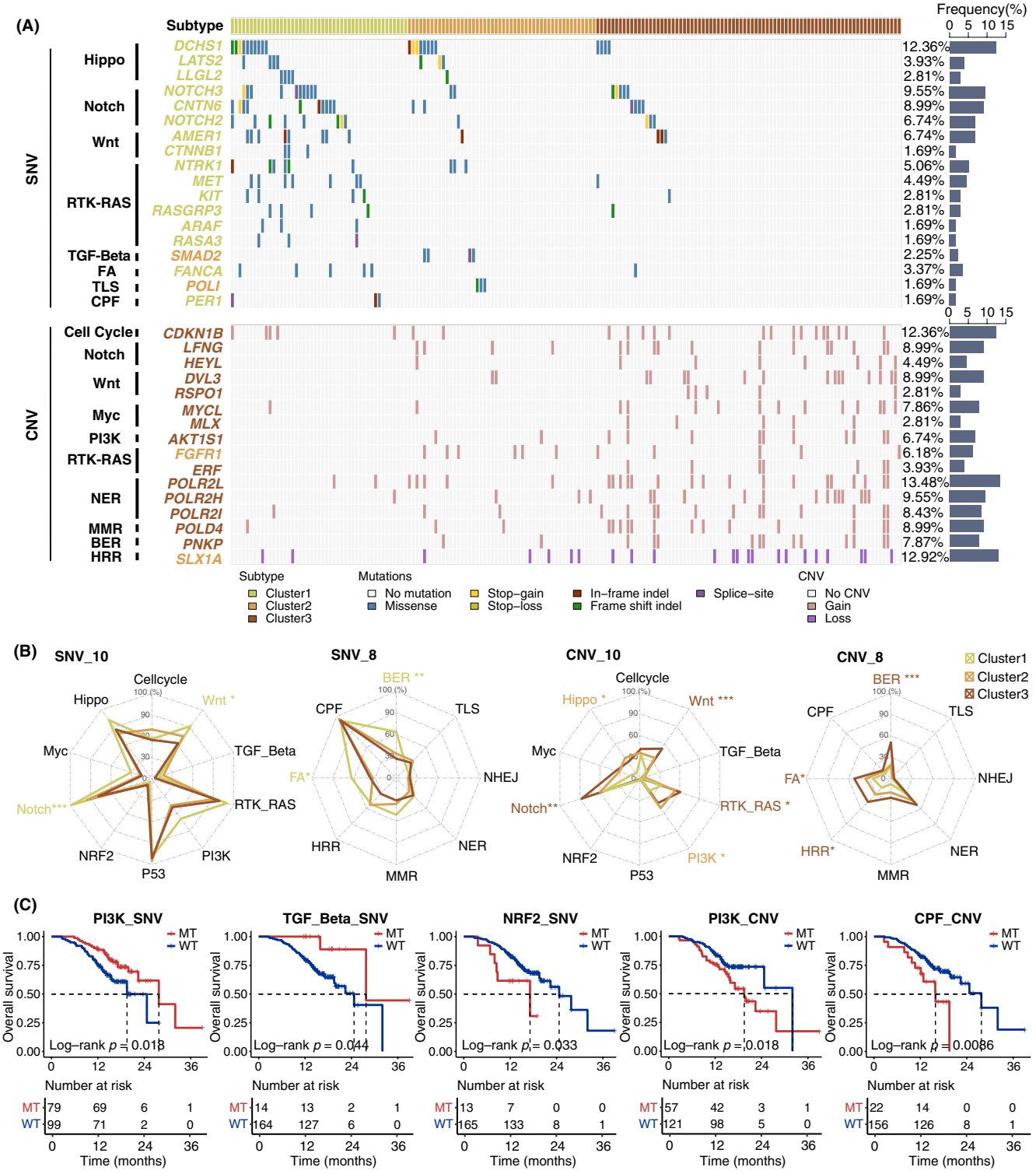

FIGURE 4 Essential pathways enriched by somatic mutation and focal copy number variation (CNV) genes among the three clusters of Chinese patients with small-cell lung cancer. (A) Differential single nucleotide variation (SNV) and focal CNV genes enriched in 10 oncogenic signaling and eight DNA damage repair (DDR) pathways. (B) Comparison of SNV and focal CNV genes enriched in 10 oncogenic signaling and eight DDR pathways among the three clusters. (C) Pathway alterations that significantly impacted overall survival. Log–rank test.

4 | DISCUSSION

Currently, there are few available drugs molecularly targeting SCLC, in contrast to NSCLC, in which genotype-directed targeted therapies have substantially improved treatments.[26] Whole-genome sequencing among Western SCLC patients has revealed that SCLC is featured by a high number of genomic mutations and complexity.[8] Despite *TP53* and *RB1* concomitant losses observed in up to almost 100% of SCLC cases, tumor heterogeneity has thwarted SCLC treatments.[8,35] Notably, SCLC personalized treatments have

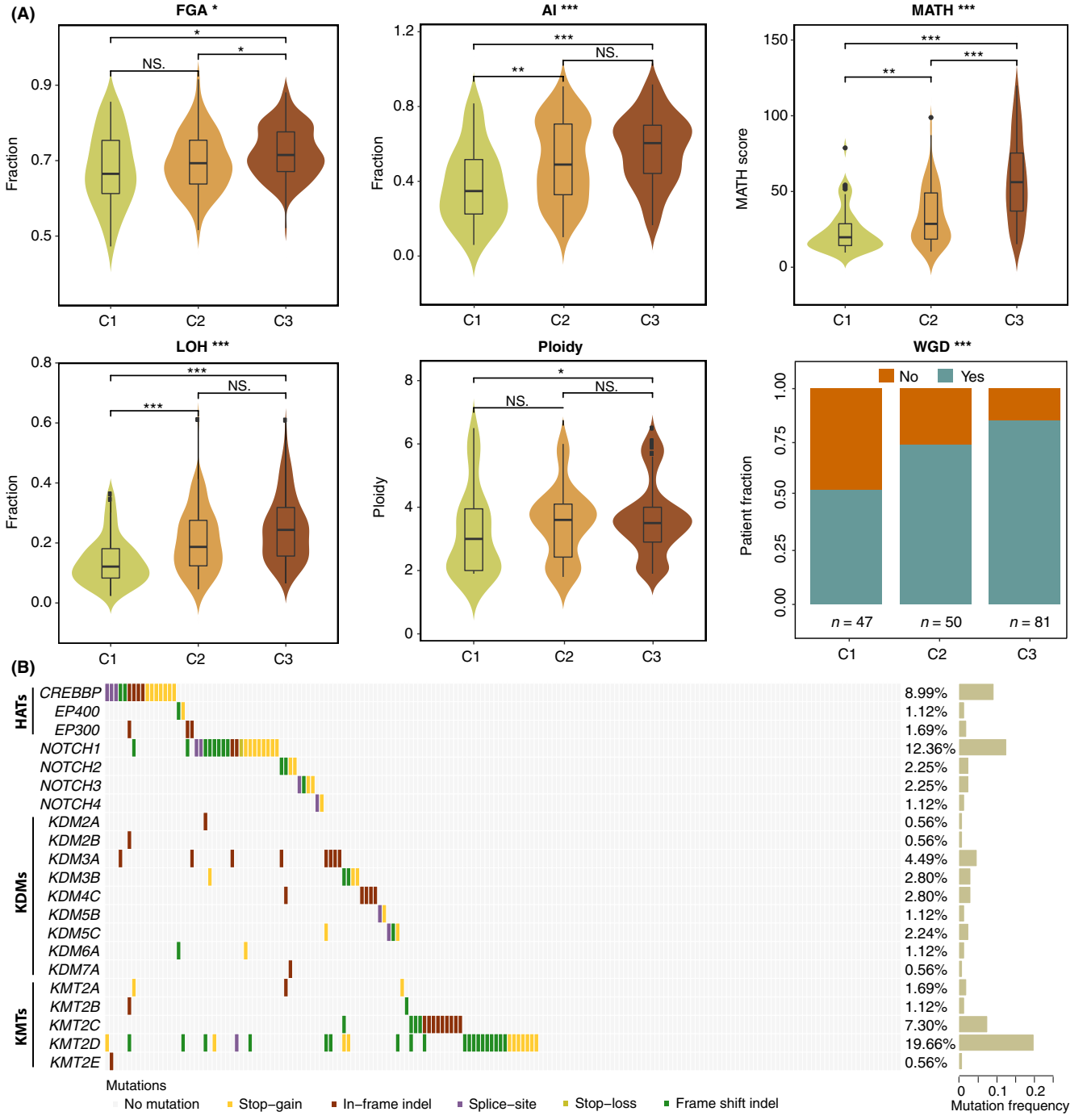

FIGURE 5 Comparison of genome instability among three clusters of Chinese patients with small-cell lung cancer. (A) Comparisons of fractions of genome altered (FGA), allelic imbalance (AI), mutant allele tumor heterogeneity (MATH), loss-of-heterozygosity regions among the whole genome (LOH), ploidy, and whole genome doubling (WGD) among the three clusters using the Wilcoxon rank–sum test (between two clusters) and the Kruskal–Wallis (trend) test. (B) Exclusive inactivation alterations trend among the genes related to genome organization. Inactivation alteration types and alteration frequencies are shown on the bottom and the right of the graph, respectively. HAT, histone acetyltransferase; KDM, lysine-specific histone demethylase; KMT, histone lysine methylation.

been highlighted in recent years.[36] Both genetically defined models and patient specimens have delineated four SCLC subtypes, determined by *ASCL1*, *NEUROD1*, *POU2F3*, and *YAP1* transcriptional regulators.[5] A subgroup, SCLC-inflamed, was further reported by Gay and is marked by the expression of multiple immune cell infiltration markers.[6] These important breakthroughs in SCLC molecular subtypes indicated that it has entered the precision medicine era.[37]

However, the previously reported SCLC subtypes based on transcription expression profiles of Caucasian populations is insufficient to comprehensively understand SCLC's genome and molecular characteristics and tailor personalized treatment to Chinese patients. Currently, there is a lack of a large population of Chinese SCLC genome research cohorts to understand its mutation characteristics. Therefore, for the first time, we successfully defined three SCLC

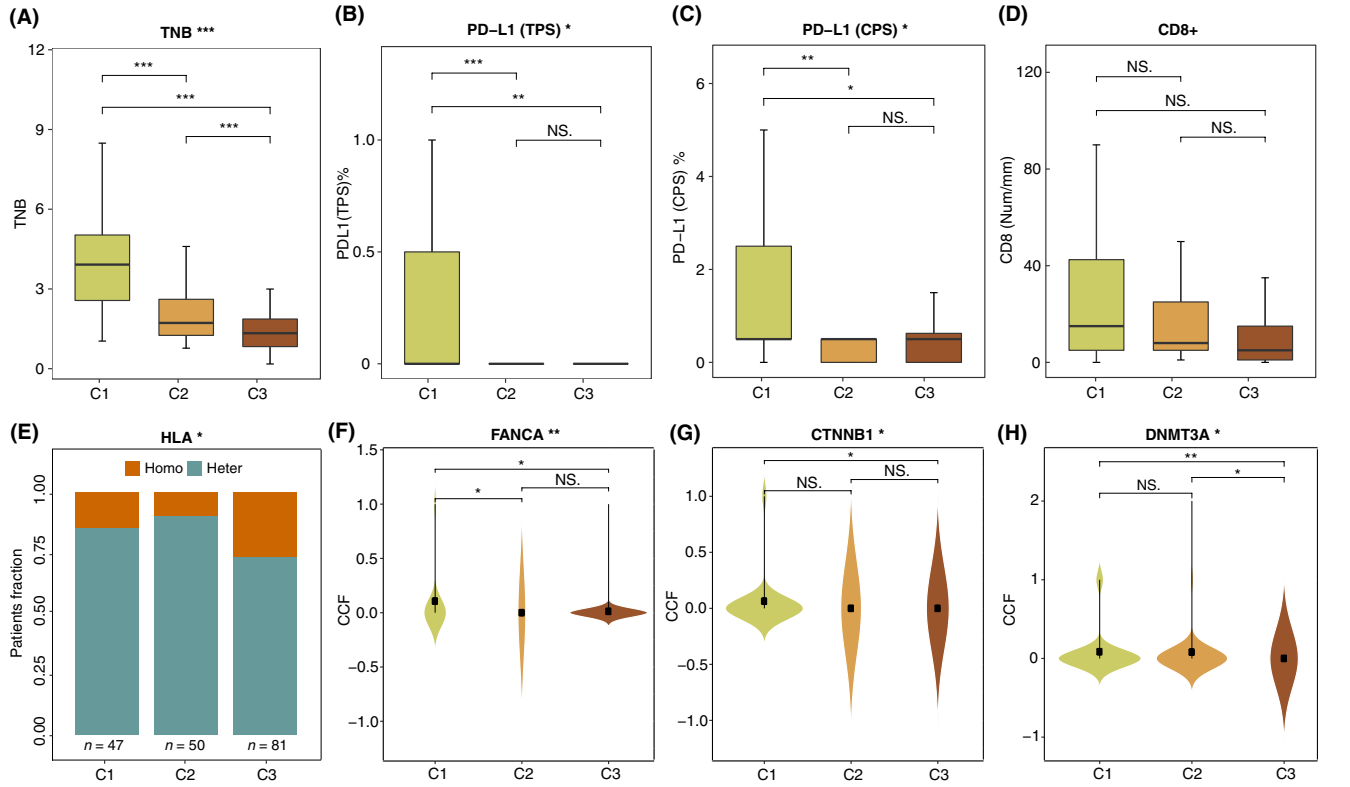

FIGURE 6 Comparison of immunotherapy-related biomarkers among three clusters of Chinese patients with small-cell lung cancer. (A–E) Comparisons of (A) tumor neoantigen burden (TNB), (B) tumor proportion score (TPS) and (C) combined positive score (CPS) of programmed cell death-ligand 1 (PD-L1) expression, (D) CD8 expression, and (E) human leukocyte antigen (HLA) heterogeneity among the three clusters. (F–H) (F) *FANCA*, (G) *CTNNB1*, and (H) *DNMT3A* gene mutation frequencies. NS., not significant; *: $p < 0.05$; **: $p < 0.01$; ***: $p < 0.001$.

subtypes from 178 specimens based on mutational signatures, comprising the largest Chinese SCLC cohort study to date. Moreover, we found distinct characteristics among the three SCLC subtypes, thereby laying the groundwork for improved SCLC management through personalized development.

Heterogeneity is prominent in SCLC and could represent a major evasion treatment mechanism, constituting a challenge in the personalized therapy era.[35,38,39] Therefore, the implementation of subtype-guided therapeutic regimens is crucial. Although several molecular studies have been performed for SCLC,[39–41] a consensus on clinically relevant subtypes, that encompasses molecular heterogeneity and can be adopted in clinical practice, has not been reported. We divided SCLC into three subtypes according to mutational signatures, and discovered that the molecular classification of SCLC was not only associated with intratumoral heterogeneity but also intimately linked with CNV and genomic stability. Also, we found a wide presence of mutually exclusive gene alterations in SCLC based on somatic mutations and CNVs, including 10 oncogenic signaling pathways and eight DDR pathways. This might be explained by the following reason: the second hit within the same pathway would bring no additional survival advantages and could result in survival disadvantage and even synthetic lethality. We noted that SCLC patients harboring PI3K and TGF-β pathway SNVs had longer OS, indicating that these patients benefited from current chemotherapies. However, patients harboring NRF2 pathway SNV, and P13K and CPF pathway CNVs did not benefit from chemotherapies. Except for these four pathways, no other pathway alterations had a relationship with OS. This phenomenon supported that high SCLC intertumoral heterogeneity could largely hinder targeted therapies' efficacy. For example, cluster 3 patients are more heterogeneous

FIGURE 7 Therapeutic vulnerability/strategies across three clusters of Chinese patients with small-cell lung cancer (SCLC). Left panel, Therapeutic strategies for the gene alteration vulnerabilities. Right panels, Essential cancer pathways, somatic mutation-related and copy number variation-related highly recurrent genes, or significantly differential genes among the three clusters selected. Genes are grouped by signaling or DNA damage repair pathways. Each gene box includes six percentage values representing the alteration frequencies of activation or inactivation among the three clusters, as explained at the bottom of the graph. The color scale bar shows the mutation frequency from 0% to 100%. Interactions between genes are indicated by arrows. *MAZ* in the star shape is the gene with high amplification frequency identified in this study and significantly affected overall survival. The table in the middle of the graph denotes different immune characteristics among the three SCLC patients clusters. BER, base excision repair; CPF, cleavage and polyadenylation factor; FA, Fanconi anemia; HAT, histone acetyltransferase; HRR, homologous recombination repair; KDM, lysine-specific histone demethylase; KMT, histone lysine methylation; MATH, mutant allele tumor heterogeneity; MMR, mismatch repair; NER, nucleotide excision repair; PD-L1, programmed cell death-ligand 1; TGF-β, transforming growth factor-β; TLS, transletion synthesis; TMB, tumor mutation burden.

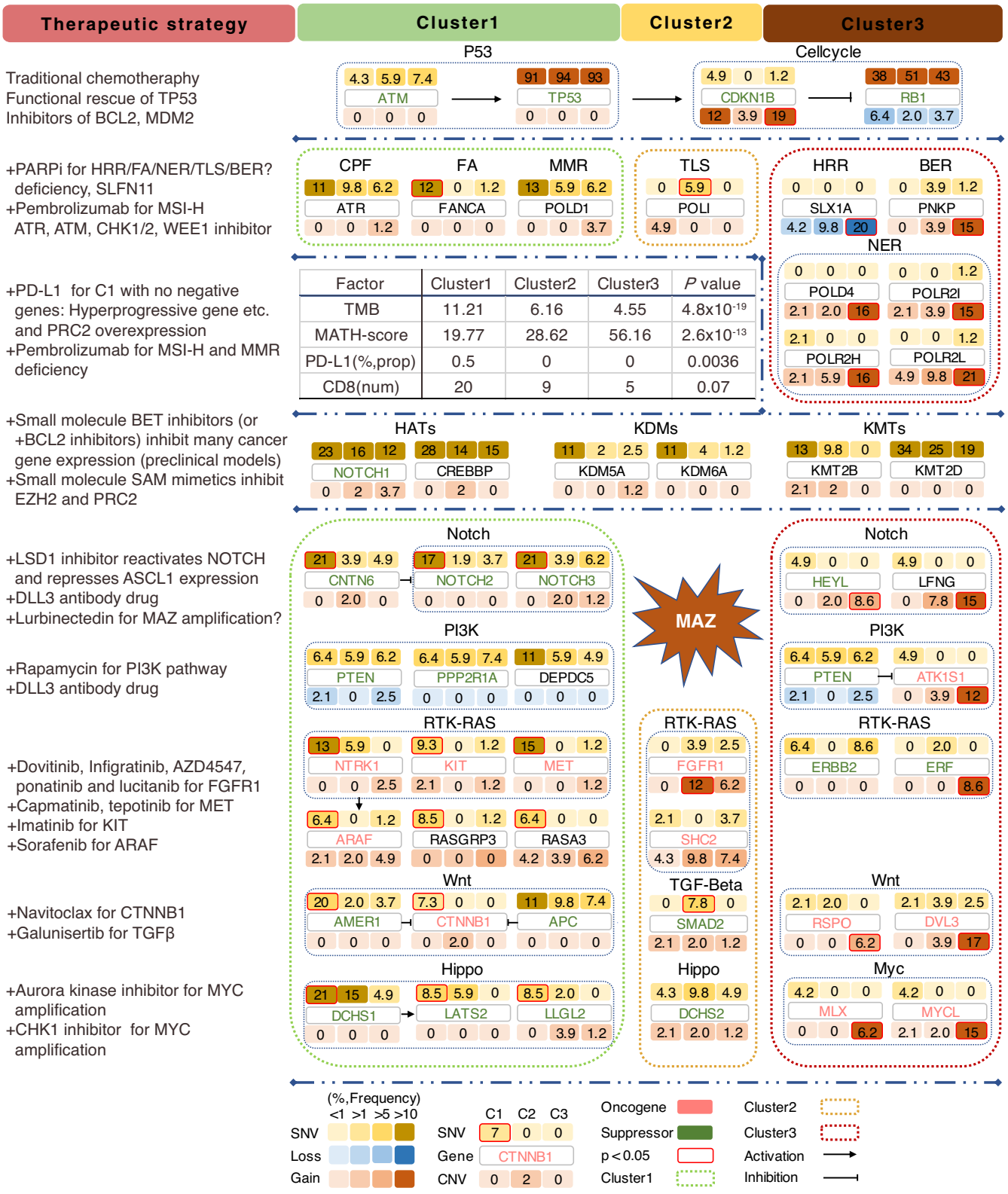

with high CNV numbers, elevated genomic stability, and shorter OS, suggesting that they might comprise recalcitrant SCLCs. Therefore, individually functional biomarker-directed drug development and targeted therapies should be undertaken in future clinical trials. Notably, although demonstrating distinct genetic mutations and pathways, the three clusters shared some key common genomic features. This suggests that the SCLC subpopulation heterogeneity might be driven by similar tumorigenesis forces during tumor evolution, such as *TP53* and *RB1* inactivation, whose function restorations are crucial for SCLC treatment.

Our study also identified other driver genes not commonly reported, such as *JUP*, *C8orf44*, *GRSF1*, and *PUM2*. Some of them evenly recurred among the three clusters in our cohort, reflecting their equivalent contribution to SCLC tumorigenesis and development. This

difference could suggest a heterogeneous SCLC genomic landscape among different races/ethnicities. This race/ethnicity difference is also found at CNV level, in which some new high-frequency amplification and deletion genes were detected. For instance, for the first time, we identified highly recurrent *MAZ* amplification and *TBC1D3* deletion, underlying their indispensable roles in SCLC development and progression among Chinese patients. Thus, molecular treatments targeting these molecular alterations should be developed.

Immunotherapy combined with chemotherapy has become the new standard for extensive-stage SCLC care.[42,43] There has been attention on predictive biomarkers that could guide ICI's use in SCLC patients. Unfortunately, no consistent predictive biomarkers have been successfully screened to date, even for conventional markers including PD-L1, TMB/TNB, and $CD8^+$ TILs. Given the benefits provided by anti-PD-1 or anti-PD-L1 Abs, the evaluation of potential biomarkers adopting multifaceted scores, such as a data combination on TILs, PD-L1, and TMB plus other factors, integrated across multiple tumor histologies, might guide future treatments.[2,44] Interestingly, in our study, cluster 1 had higher smoking-related S4 mutations, higher TMB/TNB, higher PDL-1 and CD8 expressions, and lower intratumor heterogeneity, FGA, and genome instability, suggesting cluster 1 patients might be the most appropriate subpopulation for immunotherapy. However, several immune-related negative genes were also enriched in cluster 1, which warrants the prediction of immunotherapy benefits by immune-related markers and genetic background incorporation. Moreover, prospective clinical trials should be carried out in the future to verify our inferences.

Overall, we undertook an unprecedentedly large study using WES to identify three different SCLC subtypes, which could trigger the development of rational treatments for SCLC patients. One limitation is the lack of in vitro and in vivo data supporting the rationale of the classification in the current study, which could possibly be carried out in our future studies. Additionally, we intend to clarify the differences in the immune microenvironment among the three SCLC subtypes, analyze the correlation between the previously published four genotypes based on the transcriptome and our subtypes, and undertake prospective umbrella clinical studies considering the subtypes described in our current study or target stratification. Meanwhile, the high TMB and gene alterations identified were not saturated in the SCH cohort (Figure S7). This suggested that further genomic sequencing on larger SCLC populations is required to direct an in-depth understanding of SCLC genomic features and reveal other therapeutic vulnerabilities for drug exploration.

ETHICS STATEMENT

Approval of the research protocol by an institutional review board: This study was conducted in compliance with Declaration of Helsinki principles. All procedures involving human subjects were approved by Shandong Cancer Hospital and Institute.

Informed consent: All patients included in this study provided written informed consent.

Registry and registration no. of the study/trial: Raw sequencing data were deposited in the Genome Sequencing Archive (GSA) of the China National Center for Bioinformation (CNCB) (https://ngdc.cncb.ac.cn/gsa/) under accession number subHRA001430.

Animal studies: N/A.

AUTHOR CONTRIBUTIONS

Haiyong Wang and Zhehai Wang designed and supervised the overall research. Shuangxiu Wu and Zhenzhen Li carried out data statistics and bioinformatics analysis. Chenglong Zhao made pathological confirmation and immunohistochemical analysis. Chenglong Zhao and Xiaoling Shang collected samples. Chenyue Zhang and Haiyong Wang wrote the manuscript. Zhenxiang Li and Jiamao Lin carried out survival follow-up and statistics of clinical variables. Jun Guo verified the data.

ACKNOWLEDGMENTS

This study was supported jointly by the Special Funds for Taishan Scholars Project (Grant No. tsqn201812149) and Academic Promotion Program of Shandong First Medical University (2019RC004). We thank Dianbin Mu from Shandong Cancer Hospital for his technical support in pathology, and we thank Yanxiang Zhang and Jiayan Wu from Berry Oncology Corporation for their technical support in bioinformatics.

FUNDING INFORMATION

Special Funds for Taishan Scholars Project, Grant/Award Number: tsqn201812149; Academic Promotion Program of Shandong First Medical University, Grant/Award Number: 2019RC004; China Lung Cancer Immunotherapy Research Foundation.

CONFLICT OF INTEREST

The authors declare no conflicts of interest regarding this study.

ORCID

Haiyong Wang https://orcid.org/0000-0002-0658-4479
Zhenxiang Li https://orcid.org/0000-0002-9648-8869

REFERENCES

1. Gazdar AF, Bunn PA, Minna JD. Small-cell lung cancer: what we know, what we need to know and the path forward. *Nat Rev Cancer*. 2017;17(12):725-737.
2. Iams WT, Porter J, Horn L. Immunotherapeutic approaches for small-cell lung cancer. *Nat Rev Clin Oncol*. 2020;17(5):300-312.
3. Poirier JT, George J, Owonikoko TK, et al. New approaches to SCLC therapy: from the laboratory to the clinic. *J Thorac Oncol*. 2020;15(4):520-540.
4. Khan P, Siddiqui JA, Maurya SK, et al. Epigenetic landscape of small cell lung cancer: small image of a giant recalcitrant disease. *Semin Cancer Biol*. 2020;S1044–579X(20):30240-30246.
5. Rudin CM, Brambilla E, Faivre-Finn C, Sage J. Small-cell lung cancer. *Nat Rev Dis Primers*. 2021;7(1):3.
6. Gay CM, Stewart CA, Park EM, et al. Patterns of transcription factor programs and immune pathway activation define four major subtypes of SCLC with distinct therapeutic vulnerabilities. *Cancer Cell*. 2021;39(3):346-360.e7.
7. Drapkin BJ, Rudin CM. Advances in small-cell lung cancer (SCLC) translational research. *Cold Spring Harb Perspect Med*. 2021;11(4):a038240.

8. George J, Lim JS, Jang SJ, et al. Comprehensive genomic profiles of small cell lung cancer. *Nature*. 2015;524(7563):47-53.
9. Kim KB, Dunn CT, Park KS. Recent progress in mapping the emerging landscape of the small-cell lung cancer genome. *Exp Mol Med*. 2019;51(12):1-13.
10. Gehring JS, Fischer B, Lawrence M, Huber W. SomaticSignatures: inferring mutational signatures from single-nucleotide variants. *Bioinformatics*. 2015;31(22):3673-3675.
11. Rosenthal R, McGranahan N, Herrero J, Taylor BS, Swanton C. DeconstructSigs: delineating mutational processes in single tumors distinguishes DNA repair deficiencies and patterns of carcinoma evolution. *Genome Biol*. 2016;17:31.
12. Chen J, Yang H, Teo ASM, et al. Genomic landscape of lung adenocarcinoma in east Asians. *Nat Genet*. 2020;52(2):177-186.
13. Cibulskis K, Lawrence MS, Carter SL, et al. Sensitive detection of somatic point mutations in impure and heterogeneous cancer samples. *Nat Biotechnol*. 2013;31(3):213-219.
14. Wang K, Li M, Hakonarson H. ANNOVAR: functional annotation of genetic variants from high-throughput sequencing data. *Nucleic Acids Res*. 2010;38(16):e164.
15. Szolek A, Schubert B, Mohr C, Sturm M, Feldhahn M, Kohlbacher O. OptiType: precision HLA typing from next-generation sequencing data. *Bioinformatics*. 2014;30(23):3310-3316.
16. Lawrence MS, Stojanov P, Polak P, et al. Mutational heterogeneity in cancer and the search for new cancer-associated genes. *Nature*. 2013;499(7457):214-218.
17. Martincorena I, Raine KM, Gerstung M, et al. Universal patterns of selection in cancer and somatic tissues. *Cell*. 2017;171(5):1029-1041.
18. Mermel CH, Schumacher SE, Hill B, Meyerson ML, Beroukhim R, Getz G. GISTIC2.0 facilitates sensitive and confident localization of the targets of focal somatic copy-number alteration in human cancers. *Genome Biol*. 2011;12(4):R41-R41.
19. Sanchez-Vega F, Mina M, Armenia J, et al. Oncogenic signaling pathways in the cancer genome atlas. *Cell*. 2018;173(2):321-337.
20. Knijnenburg TA, Wang L, Zimmermann MT, et al. Genomic and molecular landscape of DNA damage repair deficiency across the cancer genome atlas. *Cell Rep*. 2018;23(1):239-254.
21. Alexandrov LB, Nik-Zainal S, Wedge DC, et al. Signatures of mutational processes in human cancer. *Nature*. 2013;500(7463):415-421.
22. Jiang L, Huang J, Higgs BW, et al. Genomic landscape survey identifies SRSF1 as a key Oncodriver in small cell lung cancer. *PLoS Genet*. 2016;12(4):e1005895.
23. Umemura S, Mimaki S, Makinoshima H, et al. Therapeutic priority of the PI3K/AKT/mTOR pathway in small cell lung cancers as revealed by a comprehensive genomic analysis. *J Thorac Oncol*. 2014;9(9):1324-1331.
24. Peifer M, Fernández-Cuesta L, Sos ML, et al. Integrative genome analyses identify key somatic driver mutations of small-cell lung cancer. *Nat Genet*. 2012;44(10):1104-1110.
25. Rudin CM, Durinck S, Stawiski EW, et al. Comprehensive genomic analysis identifies SOX2 as a frequently amplified gene in small-cell lung cancer. *Nat Genet*. 2012;44(10):1111-1116.
26. Sabari JK, Lok BH, Laird JH, Poirier JT, Rudin CM. Unravelling the biology of SCLC: implications for therapy. *Nat Rev Clin Oncol*. 2017;14(9):549-561.
27. Zhao H, Zhang L, Zhang Y, et al. Calmodulin promotes matrix metalloproteinase 9 production and cell migration by inhibiting the ubiquitination and degradation of TBC1D3 oncoprotein in human breast cancer cells. *Oncotarget*. 2017;8(22):36383-36398.
28. Luo W, Zhu X, Liu W, et al. MYC associated zinc finger protein promotes the invasion and metastasis of hepatocellular carcinoma by inducing epithelial mesenchymal transition. *Oncotarget*. 2016;7(52):86420-86432.
29. Wang Z, Zhao J, Wang G, et al. Comutations in DNA damage response pathways serve as potential biomarkers for immune checkpoint blockade. *Cancer Res*. 2018;78(22):6486-6496.
30. Oswald F, Täuber B, Dobner T, et al. p300 acts as a transcriptional coactivateor for mammalian Notch-1. *Mol Cell Biol*. 2001;21(22):7761-7774.
31. Lim JU, Kang HS. A narrative review of current and potential prognostic biomarkers for immunotherapy in small-cell lung cancer. *Ann Transl Med*. 2021;9(9):809.
32. Remon J, Aldea M, Besse B, et al. Small cell lung cancer: a slightly less orphan disease after immunotherapy. *Ann Oncol*. 2021;32(6):698-709.
33. Chowell D, Morris LGT, Grigg CM, et al. Patient HLA class I genotype influences cancer response to checkpoint blockade immunotherapy. *Science*. 2018;359(6375):582-587.
34. Shen J, Ju Z, Zhao W, et al. ARID1A deficiency promotes mutability and potentiates therapeutic antitumor immunity unleashed by immune checkpoint blockade. *Nat Med*. 2018;24(5):556-562.
35. Stewart CA, Gay CM, Xi Y, et al. Single-cell analyses reveal increased intratumoral heterogeneity after the onset of therapy resistance in small-cell lung cancer. *Nat Cancer*. 2020;1:423-436.
36. Drapkin BJ, Farago AF. Unexpected synergy reveals new therapeutic strategy in SCLC. *Trends Pharmacol Sci*. 2019;40(5):295-297.
37. Frese KK, Simpson KL, Dive C. Small cell lung cancer enters the era of precision medicine. *Cancer Cell*. 2021;39(3):297-299.
38. Simpson KL, Stoney R, Frese KK, et al. A biobank of small cell lung cancer CDX models elucidates inter- and intratumoral phenotypic heterogeneity. *Nat Cancer*. 2020;1:437-451.
39. Arriola E, Cañadas I, Arumí M, Rojo F, Rovira A, Albanell J. Genetic changes in small cell lung carcinoma. *Clin Transl Oncol*. 2008;10(4):189-197.
40. Mollaoglu G, Guthrie MR, Böhm S, et al. MYC drives progression of small cell lung cancer to a variant neuroendocrine subtype with vulnerability to Aurora kinase inhibition. *Cancer Cell*. 2017;31(2):270-285.
41. Baine MK, Hsieh MS, Lai WV, et al. SCLC subtypes defined by ASCL1, NEUROD1, POU2F3, and YAP1: a comprehensive immunohistochemical and histopathologic characterization. *J Thorac Oncol*. 2020;15(12):1823-1835.
42. Horn L, Mansfield AS, Szczęsna A, et al. First-line Atezolizumab plus chemotherapy in extensive-stage small-cell lung cancer. *N Engl J Med*. 2018;379(23):2220-2229.
43. Paz-Ares L, Dvorkin M, Chen Y, et al. Durvalumab plus platinum-etoposide versus platinum-etoposide in first-line treatment of extensive-stage small-cell lung cancer (CASPIAN): a randomised, controlled, open-label, phase 3 trial. *Lancet*. 2019;394(10212):1929-1939.
44. Ott PA, Bang YJ, Piha-Paul SA, et al. T-cell-inflamed gene-expression profile, programmed death ligand 1 expression, and tumor mutational burden predict efficacy in patients treated with pembrolizumab across 20 cancers: KEYNOTE-028. *J Clin Oncol*. 2019;37(4):318-327.

SUPPORTING INFORMATION

Additional supporting information can be found online in the Supporting Information section at the end of this article.

How to cite this article: Wang H, Wu S, Li Z, et al. Molecular subtyping of small-cell lung cancer based on mutational signatures with different genomic features and therapeutic strategies. *Cancer Sci*. 2023;114:665-679. doi: 10.1111/cas.15606